ISSN 2616-5767 Vol.4, Issue 8: 64-80, DOI: 10.25236/AJETS.2021.040808

Analysis of Crack Stress Intensity Factor of Coke Drum under Thermal Stress by Weight Function Method

Zhiwen Wang

School of Mechanics and Construction Engineering, Key Laboratory of Disaster Forecast and Control in Engineering, Ministry of Education of China, Jinan University, Guangzhou 510632, China
twangzhiwen@163.com

Abstract: *The coke drum undergoes severe cyclic temperature changes during service, and it is prone to ring cracks. Based on linear elastic fracture mechanics, this paper uses the weight function method to solve the stress intensity factor of the coke drum with circumferential cracks in a two-dimensional transient temperature field. Based on the edge crack stress intensity factor of the finite width slab, the weight function of the circumferential crack stress intensity factor of the cylindrical shell is deduced according to the self-consistent condition of the crack stress intensity factor and the curvature of the crack mouth opening. Using the weight function obtained, the stress intensity factors of different depth cracks in the coke drum are analyzed, and compared with the results of the literature, the agreement is good. Then, the influence of different liquid rise rates and different thermal conductivity coefficients in the coke drum on the crack stress intensity is analyzed. The influence of factors. The research in this paper lays a theoretical foundation for the prediction of crack propagation and remaining life of the coke drum.*

Keywords: *coke drum, two-dimensional transient temperature field, cylindrical shell, weight function method, stress intensity factor*

1. Instruction

The coke drum, also known as the thermal cracking reactor, is one of the important equipment of the delayed coking unit. Its function is to decarburize high-residual-carbon oil products so that they can be smoothly converted into other high-value products. The structure of the coke drum is relatively simple. Generally, a plate-welded structure is adopted. Its main part can be regarded as a cylindrical shell, with a conical bottom at the bottom and a semi-ellipsoidal head at the top, as shown in Figure 1. However, in actual production, the coke drum is usually alternately placed in the high temperature environment during the coking period and the cooling environment during the decoking period for a long time, causing cold and heat fatigue problems. Therefore, after a period of application, it is easy to produce harmful defects such as cracks. In order to promote the development of the productivity of the refinery, the characteristics of the cracks in the coke drum should be deeply analyzed. Ignoring the welds between the sections of the coke drum, as well as the tapered back cover at the bottom and the semi-ellipsoidal head at the top, the main body of the coke drum can be seen as a cylindrical shell in the form of Figure 2. Therefore, the circumferential cracking of the coke drum body can be simplified to the circumferential cracking of the cylindrical shell under the action of heat load for research.

In the 1970s, many scholars began to study the stress intensity factor of cylindrical shells with circumferential cracks. Among them, the problem of cylindrical shells with circumferential cracks on the inner wall under axial load has formed many research methods, the main methods involved include finite element method, weight function method, boundary element method and so on. Glinka and Shen[1] proposed a general form of the weight function for calculating the stress intensity factor of mode I based on the opening displacement of the crack tip and the reference stress intensity factor, which laid a certain theoretical foundation for subsequent research. Nied and Erdogan[2] proposed an accurate solution method for cylindrical shells under uniform tensile load, and gave the numerical results of the stress intensity factor of mode I cracks, but this method is only applicable to $0.1 \le \gamma \le 1, 0 \le \beta \le 0.6$ (γ is the ratio of inner and outer diameters, β is the ratio of crack depth to shell thickness). Petersilge and Varfolomeyev[3] used the boundary element method to obtain the simpler weight function of the problem, and their solutions can be respectively applied to $0.9 \le \gamma \le 1, 0 \le \beta \le 0.7$ and $0.1 \le \gamma \le 1, 0 \le \beta \le 0.8$, And the error is less than 3%. Mettu and Forman[4] used the finite element method to derive the weight function of the stress intensity factor when the inner and outer surfaces of the thin-walled cylindrical shell contain circular cracks based on the opening displacement of the crack surface under uniform loading. Nabavi and Ghajar[5] derived a general expression for calculating the stress intensity factor of a cylindrical shell with circumferential cracks through the definition of the weight function. The coefficients were obtained by fitting using the finite element method. The solution is suitable for the ratio of inner and outer diameters. In the case of 0.5 to 0.9. Tuo Xuan[6] studied the fracture mechanics behavior of a thin-walled cylindrical shell with circumferential cracks, and analyzed the relationship between the stress intensity factor K and the J integral in the case of a small yield.

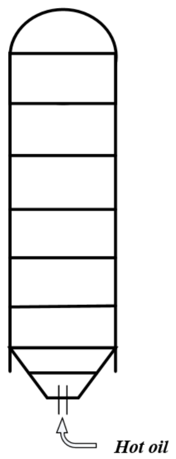

Fig.1 The plate-welded structure of the coke drum

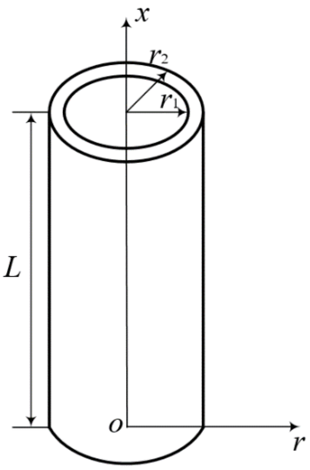

Fig.2 Simplified model of coke drum

Compared with the research on the cylindrical shell under mechanical load, the research on the stress intensity factor of the cylindrical shell crack under the one-dimensional or two-dimensional transient temperature field is much less. Nied and Erdogan[7] analyzed the stress intensity factor when the inner surface of a cylindrical shell with annular cracks on the inner wall is subjected to cooling. According to the temperature field and stress field when there is no crack, the obtained thermal stress is reversely acted on the crack surface, and the value is kept consistent, and the stress intensity factor at the time of the crack is derived, and then the stress intensity factor in these two cases is superimposed Come to get the answer to the question. Jayadevan[8] used the method of finite element analysis to analyze the stress intensity factor of circumferential cracks on the inner wall of a cylindrical shell subjected to convective cooling, and calculated the stress intensity factor through J integral. Jones[9] also analyzed the problem of a cylindrical shell with circumferential cracks under thermal load, and obtained the function of the stress intensity factor and the crack depth through the impulse response method. Meshii and Watanabe[10-15] conducted a lot of research on cylindrical shells with circumferential cracks, including periodic temperature changes and various linear and nonlinear radial temperature fields. The function method and superposition principle consider the problem as a finite-length edge cracked beam, obtain the corresponding stress intensity factor expression, and analyze the influence of the length of the cylindrical shell on the stress intensity factor. Nabavi and Shahani[16] calculated the transient thermal stress intensity factors of the deepest and surface points of the axial semi-elliptical surface cracks of a cylindrical shell under thermal shock, assuming that the thermal boundary conditions acting on the inner surface of the cylindrical shell under compression change with time. The precise analytical solution of the weight function is derived and integrated to calculate the transient thermal stress intensity factor. Eshraghi[17] et al. used a non-Fourier hyperbolic heat conduction model to calculate the transient temperature distribution of a functionally graded cylindrical shell, transformed the control differential equation into an integral equation in the Laplace domain, and derived the solution of the transient temperature and stress distribution of a crackless cylindrical shell. , And then use the weight function method similar to that derived by Nabavi and Ghajar[7] to derive the corresponding thermal stress intensity factor of the cylindrical shell I-shaped circumferential crack. Fu[18] et al. also used the non-Fourier heat conduction theory to study the fracture behavior of a hollow cylinder with inner edge circumferential cracks under thermal boundary conditions. By ignoring the thermoelastic coupling and inertial effects, they obtained the The one-dimensional temperature field and axial thermal stress of the cracked hollow cylinder, and then the solution of the stress intensity factor of the type I crack in the cylinder system is derived by the superposition method.

In summary, the most common method for calculating the stress intensity factor of circumferential cracks in cylindrical shells is the finite element method or the weight function method, or a combination of the two. The finite element method requires a lot of meshing, which is tedious and time-consuming. In comparison, the weight function method is simple and convenient to solve the crack stress intensity factor, and the result is more accurate. The weight function is only related to the physical geometry of the crack body, and has nothing to do with the load form, so for the crack body, only After the weight function is obtained by applying a simple load form, the stress on the imaginary crack surface when there is no crack is solved. Then the stress intensity factor of the crack body under any load condition can be obtained by integrating the stress and the weight function.

The problem of circumferential cracks in coke drums in a two-dimensional transient temperature field mainly involves type I cracks. In view of the axial symmetry of the problem, this paper is based on the analytical solution of the stress intensity factor of the edge crack of the finite width slab under the uniform load of the crack surface as the reference load stress intensity factor, using the self-consistent condition of the reference stress intensity factor of the crack and The crack opening displacement conditions are used to derive the weight function of the circumferential crack stress intensity factor of the cylindrical shell; then, using the analytical solution of the two-dimensional transient thermoelastic field of the coke drum established by Ning Zhihua and Liu Renhuai[19-20], the weight function method is used The thermal stress intensity factor when the coke drum contains circumferential cracks is calculated, which lays a theoretical foundation for the subsequent crack propagation and residual strength prediction of the coke drum.

2. Thermoelastic field of coke drum

2.1 The answer to the thermoelastic field

The body of the coke drum can be simplified as a cylindrical shell as shown in Figure 2. Regarding the answer to the thermoelastic field of the coke drum, consider the temperature field during the oil or water inlet phase of the coke drum. At this stage, the liquid rises from the bottom of the drum at a constant speed, and the liquid below the liquid level exchanges heat with the inner wall of the drum, and there is also heat exchange between the inner wall of the drum and the gas in the drum above the liquid level. Ning Zhihua and Liu Renhuai[19-20] regarded the entire temperature field of the drum as the upper and lower segments with the liquid surface as the boundary, and gave an analytical solution to the two-dimensional transient thermoelastic field of the coke drum. According to the boundary conditions, temperature, displacement and internal force continuity conditions, the thermoelastic field of the coke drum wall is solved.

The temperature fields of the upper and lower sections of the coke drum are respectively expressed as $T_d(x,r,t), T_u(x,r,t)$, and the solution of the transient temperature field of the coke drum is as follows [20]:

$$T_d(x,r,t) = T_f + \sum_{m=0}^{\infty}\sum_{n=1}^{\infty} B_{mn}[J_0(d_n r) + F_n Y_0(d_n r)]\cos(\frac{m\pi}{L}x)\exp[-a(d_n^2 + \frac{m^2\pi^2}{L^2})(t - \frac{x}{v})] \quad (1)$$

$$T_u(x,r) = T_s + \sum_{n=1}^{\infty} A_n'[J_0(d_n' r) + F_n' Y_0(d_n' r)][\exp(d_n' x) + G_n \exp(-d_n' x)] \quad (2)$$

Where Tf is the temperature of the liquid in the drum, T_s is the gas temperature in the upper section of the drum, a is the thermal diffusivity of the coke drum wall, v is the liquid rising speed, L is the height of the coke drum, $J_i, Y_i (i = 0,1)$ are Bessel functions of order 0 and order 1 of the first and second types, d_n, d_n' are the characteristic roots that satisfy the boundary conditions of the coke drum wall heat conduction, see reference [20]:

$$F_n = -J_1(d_n r_2)/Y_1(d_n r_2),\ \ F_n' = -J_1(d_n' r_2)/Y_1(d_n' r_2),\ \ G_n = e^{2d_n' L} \quad (3)$$

Where r2 is the radius of the outer wall of the coke drum.

According to reference [20], the coordinate system shown in Fig. 3 is established, and the radial displacement solution of the upper and lower wall of the coke drum can be expressed as [20]:

$$w = e^{-\eta\rho}(c_1 \cos\eta\rho + c_2 \sin\eta\rho) + e^{\eta\rho}(c_3 \cos\eta\rho + c_4 \sin\eta\rho) + w^* \quad (4)$$

Among them, $\rho = \frac{x}{R}$, R is the radius of the middle surface of the coke drum, c_i is a constant, and w^* is the special solution of the displacement of the upper and lower ends of the coke drum. See reference [20] for details.

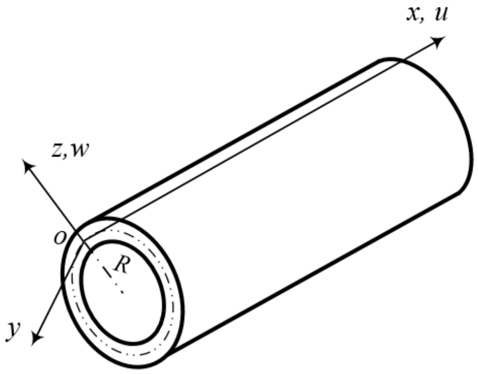

Fig.3 Cylindrical shell coordinates

2.2 Results of thermoelastic field

The geometric parameters and material parameters of the coke drum are selected as shown in Table 1 and Table 2.

Table 1 Material and geometric parameters of coke drum

	Feed filling step	Water quench step
Initial temperature of drum wall T^0/ ºC	320	330
Liquid temperature T_f/ ºC	495	70
Heat exchange coefficient h / (W/(m^2.K))	1700	2500
Liquid rising speed v/ (mm/s)	1.0	2.0

Table 2 Operating parameters

Coke drum operating parameters	
Mass Density ρ/(kg/m^3)	7833
Specific heat capacity C / (J/(kg.K))	470.84
Thermal conductivity k / (W/ (m.K))	51.068
Elastic Modulus E / (GPa)	193
Poisson's ratio u	0.28
Thermal expansion coefficient α ($10^{-6}K^{-1}$)	1.088
Drum Height L/m	30
Inner radius r_1/m	2.7
Outer radius r_2/m	2.728

Using equations (1), (2) and (4), the transient temperature field and thermoelastic field of the coke drum wall can be calculated.

During the oil and water intake phases, the liquid level continues to rise, causing the boundary conditions of the transient temperature field to also change. In the Abaqus analysis, the film subprogram is used to simulate the change of the liquid interface, so that the liquid below the liquid level exchanges heat with the coke drum wall, while the coke drum wall above the liquid level is constantly exchanging heat with the air. When the liquid level reaches a certain height, the transient temperature field of the coke drum wall below the liquid level will gradually become stable. In this paper, the coke drum temperature field and thermal stress-strain field analysis adopts an indirect coupling method. The temperature field analysis uses a four-node linear axisymmetric heat transfer quadrilateral element, and the thermal stress analysis uses a corresponding four-node axisymmetric thermal coupling quadrilateral element. Bidirectional linear displacement, bidirectional linear temperature. The finite element analysis is divided into two steps. The first step is to calculate the temperature field distribution of the coke drum body, and the second step is to analyze the thermal stress-strain field according to the temperature distribution.

ISSN 2616-5767 Vol.4, Issue 8: 64-80, DOI: 10.25236/AJETS.2021.040808

The following assumes that the coke drum inlet water cooling time is 2000s, the water surface rising speed is 2mm/s, and the rising height is up to 4m. The calculation results are shown in Figure 4 to Figure 8.

It can be seen from Figure 4 to Figure 8 that the calculation results of Ning Zhihua and Liu Renhuai[19-20] on the thermoelastic field of the coke drum are basically consistent with the finite element numerical results in this paper. Figures 4 and 5 reflect that the coke drum has been cooled to 330 ℃ by high-temperature steam before the water cooling coke. After the cooling water is injected into the coke drum body from the bottom, the coke drum wall temperature drops rapidly as the cooling water rises. Near the liquid level, The temperature changes exponentially. As the cooling water surface rises, the coke drum wall forms a stable temperature field, which rises together with the water surface.

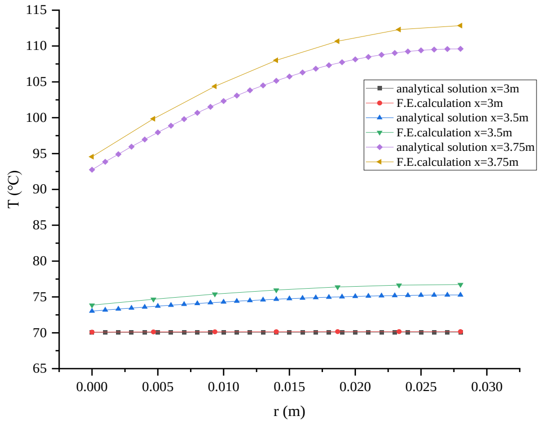

Fig.4 Radial temperature distribution of coke drum wall

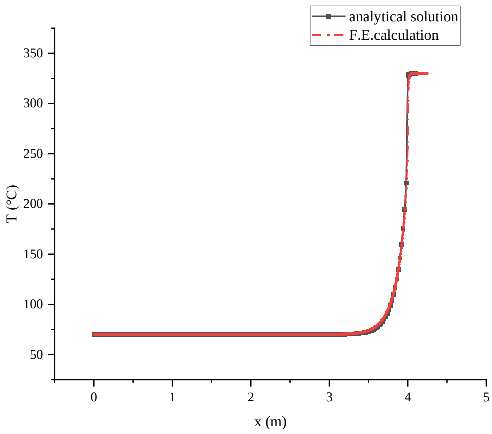

Fig.5 Axial temperature distribution on the inner wall of coke drum

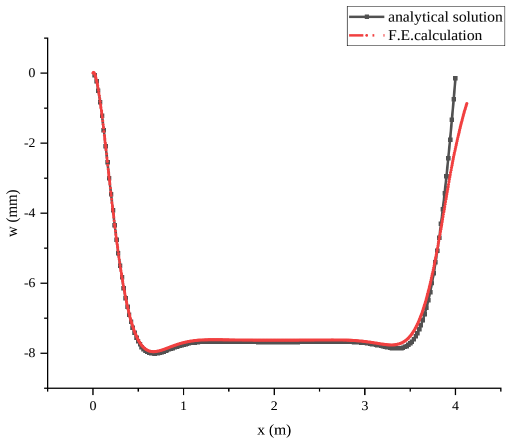

Fig.6 The axial displacement distribution of the inner wall of the coke drum

ISSN 2616-5767 Vol.4, Issue 8: 64-80, DOI: 10.25236/AJETS.2021.040808

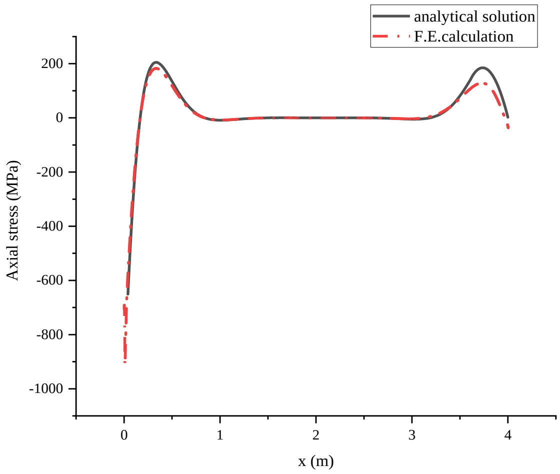

Fig.7 Axial stress distribution on the inner wall of coke drum

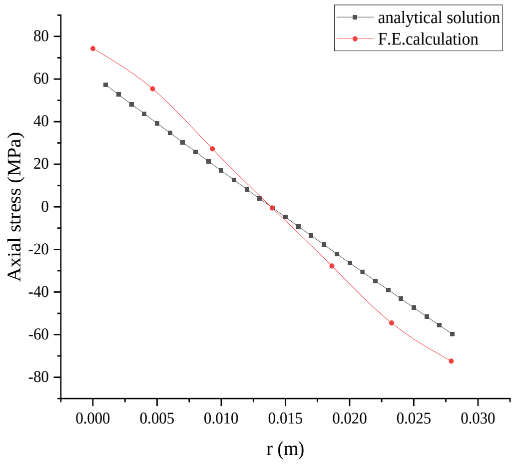

Fig.8 The radial distribution of the axial stress of the coke drum(x=3.5m)

Figures 6 and 7 respectively show the axial displacement and axial stress distribution of the inner wall of the coke drum. It can be seen from the figure that the radial displacement and axial stress peaks of the coke drum appear at about 0.5m below the liquid surface in the water inlet cooling stage. This is because the temperature gradient near the liquid surface changes greatly, resulting in greater thermal stress. Figure 8 shows the distribution of axial stress along the radial direction at the height of the coke drum at 3.5m. At this moment, the inner wall of the coke drum is stretched while the outer wall is compressed, and the stress is approximately symmetrically distributed along the middle of the wall.

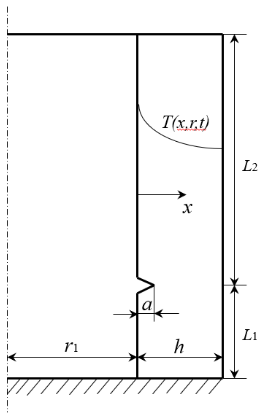

Fig.9 Coke drum with a axisymmetric

3. Weight function of cracks in coke drum

Consider the circumferential crack of the coke drum, as shown in Figure 9, there is a circumferential crack at the height L1, and the crack depth is a. Due to the symmetry of the problem, it can be regarded as an I-type crack problem in a two-dimensional transient temperature field.

The general expression of the stress intensity factor *K* is:

$$K = f\sigma\sqrt{\pi a} \tag{5}$$

Where f is the dimensionless stress intensity factor, σ is the reference stress, and a is the crack length.

Since the problem in question is axisymmetric, it can be solved by the two-dimensional weight function method. When using the two-dimensional weight function method to solve, K can be calculated by the following formula[12]:

$$K = \int_0^a \frac{R_i + x}{R_i + a}\sigma(x)m(a,x)dx \tag{6}$$

Where R_i is the inner radius of the cylindrical shell and $m(a,x)$ is the weight function. The method using the superposition principle is based on the displacement and load of the crack body boundary, or the stress distribution of various internal stresses on the imaginary crack surface, and its solution has nothing to do with the crack. Equation (7) shows that as long as the weight function $m(a,x)$ of the crack body is known, when the load $\sigma(x)$ on any crack surface acts, the crack stress intensity factor can be obtained by the integral of the stress and the weight function. The weight function is only related to the physical geometry of the cracked body, not to the load form.

The concept of weight function was proposed by Buechner[21] in 1970, and Rice[22] proposed a simple formula for solving the weight function in 1972:

$$m(a,x) = \frac{H}{K_r(a)}\frac{\partial u_r(a,x)}{\partial a} \tag{7}$$

Where H is a parameter related to the stress state, $H = E$ in the plane stress state, $H = E/(1-\mu^2)$ in the plane strain state; $K_r(a)$ is the reference stress intensity factor, and $u_r(a,x)$ is the opening displacement of the crack surface under the reference load.

In the case of axial symmetry, the circumferential cracks of the coke drum are similar to the edge cracks of the finite width slats. The analytical expression of the stress intensity factor of a single edge crack of a finite-width slab under uniform load on the crack surface is [23]:

$$K_r(a) = f_r(a)\sigma\sqrt{\pi a} \tag{8}$$

Where $f_r(a)$ is the dimensionless reference stress intensity factor for edge cracks of finite width slats.

$$f_r(a) = [1.1214 - 1.6349\frac{a}{t} + 7.3168\left(\frac{a}{t}\right)^2 - 18.7746\left(\frac{a}{t}\right)^3 + 31.8028\left(\frac{a}{t}\right)^4 - 33.2295\left(\frac{a}{t}\right)^5 + 19.1286\left(\frac{a}{t}\right)^6 - 4.609\left(\frac{a}{t}\right)^7]/(1-\frac{a}{t})^{3/2} \tag{9}$$

In the above formula, a is the depth of the crack and t is the width of the slat.

Under the condition of known reference load, the formula given by Glinka and Shen[1] can be used to calculate the opening displacement of mode I crack, namely:

$$u_r(a,x) = \frac{\sigma a}{\sqrt{2}H}\sum_{i=1}^{I} F_i(a)(1-\frac{x}{a})^{i-1/2} \tag{10}$$

When $x \to a$, the displacement near the crack tip can be calculated using the following formula:

ISSN 2616-5767 Vol.4, Issue 8: 64-80, DOI: 10.25236/AJETS.2021.040808

$$u_r\left(a,x\right)=\frac{4K_r(a)}{H}\left(\frac{a-x}{2\pi}\right)^{1/2} \tag{11}$$

The calculation of $Fi(a)$ in equation (10) is discussed below.

$F_1(a)$ can be expressed as [1]:

$$F_1\left(\mathrm{a}\right)=4f_r\left(a\right) \tag{12}$$

Fi(a), (i=2,3,...,I) can be determined by the following conditions[24]:

(1)Self-consistent condition of crack stress intensity factor

When the weight function is applied to the reference load σ_0 itself, the resulting stress intensity factor should be the same as the stress intensity factor under the original reference load, that is:

$$K_r=\int_0^a\sigma_0 m\left(a,x\right)dx=\int_0^a\sigma_0\frac{H}{K_r}\frac{\partial u_r\left(a,x\right)}{\partial a}dx \tag{13}$$

Simplify to get:

$$\int_0^a K_r^{\ 2}da=H\int_0^a\sigma_0 u_r\left(a,x\right)dx \tag{14}$$

Substituting equation (10) into equation (14), we can get:

$$\sqrt{2}\pi\int_0^a s?f_r^{\ 2}\left(s\right)ds=a^2\int_0^a\frac{\sigma_r\left(x\right)}{\sigma}\sum_{i=1}^{I}F_i\left(a\right)\left(1-\frac{x}{a}\right)^{i-1/2}dx \tag{15}$$

Introduce a new function $\emptyset(a)$:

$$\varnothing\left(a\right)=\frac{1}{a^2}\int_0^a s\, f_r^{\ 2}\left(s\right)ds \tag{16}$$

The reference load is a polynomial distribution along the crack surface, namely:

$$\sigma_r\left(x\right)=\sum_{m=0}^{M}S_m x^m$$

$$E_j\left(a\right)=\sum_{m=0}^{M}\frac{2^{m+1}m!S_m a^m}{\prod_{k=0}^{m}\left(1+2j+2k\right)} \tag{17}$$

When the reference load is linear, formula (15) can be rewritten as:

$$\sqrt{2}\pi\varnothing\left(a\right)=\sum_{i=1}^{I}F_i\left(a\right)E_i\left(a\right) \tag{18}$$

Where $E_i(a)$ is a term related to the load. When the reference load is a uniform load applied on the crack surface:

$$E_i\left(a\right)=\frac{2}{2i+1} \tag{19}$$

(2)The curvature at the crack mouth is 0

When $x = 0$:

$$\frac{\partial^2 u\left(a,x\right)}{\partial x^2}=0 \tag{20}$$

Substituting equation (10) into equation (20), we get:

ISSN 2616-5767 Vol.4, Issue 8: 64-80, DOI: 10.25236/AJETS.2021.040808

$$\sum_{i=1}^{i}(2i-1)(2i-3)F_i(a)=0 \tag{21}$$

Finally, from equations (16), (18) and (21), we can get:

$$F_2(\mathrm{a})=\frac{F_1(\mathrm{a})E_3(\mathrm{a})+15F_1(\mathrm{a})E_1(\mathrm{a})-15\sqrt{2}\pi\varnothing(\mathrm{a})}{3E_3(\mathrm{a})-15E_2(a)}$$

$$F_3(\mathrm{a})=\frac{-F_1(\mathrm{a})E_2(\mathrm{a})-3F_1(\mathrm{a})E_1(\mathrm{a})+3\sqrt{2}\pi\varnothing(\mathrm{a})}{3E_3(\mathrm{a})-15E_2(a)} \tag{22}$$

The opening displacement of the crack surface is finally obtained as:

$$u(a,x)=\frac{\sigma a}{\sqrt{2}H}\left[F_1(\mathrm{a})\left(1-\frac{x}{a}\right)^{\frac{1}{2}}+F_2(\mathrm{a})\left(1-\frac{x}{a}\right)^{\frac{3}{2}}+F_3(\mathrm{a})\left(1-\frac{x}{a}\right)^{5/2}\right] \tag{23}$$

The expression of the weight function is:

$$\begin{aligned}m(a,x)=\frac{4}{f_r(a)\sqrt{2\pi a}}\sum_{i=1}^{3}[F_i(a)\left(1-\frac{x}{a}\right)^{i-1/2}+aF_i^{'}(a)(1-\frac{x}{a})^{i-1/2}\\-(i-1/2)F_i(a)xa^{-1}(1-\frac{x}{a})^{i-3/2}]\}\end{aligned} \tag{24}$$

The expression of each function in the formula is as follows:

$$\varnothing^{'}(a)=-\frac{2}{a^3}\int_0^a s\,f_r^{\,2}(s)ds+\frac{f_r^{\,2}(a)}{a}$$

$$E_i^{'}(a)=0$$

$$F_1^{'}(a)=4f_{\mathrm{r}}^{'}(a)$$

$$F_2^{'}(a)=\frac{\left[15\sqrt{2}\pi\varnothing^{'}(a)-15E_1(\mathrm{a})F_1^{'}(a)-F_1^{'}(a)E_3(\mathrm{a})\right]\left[15E_2(a)-3E_3(\mathrm{a})\right]}{\left[3E_3(\mathrm{a})-15E_2(a)\right]^2}$$

$$F_3^{'}(a)=\frac{\left[-3\sqrt{2}\pi\varnothing^{'}(a)+E_2(\mathrm{a})F_1^{'}(a)+3F_1^{'}(a)E_1(\mathrm{a})\right]\left[15E_2(a)-3E_3(\mathrm{a})\right]}{\left[3E_3(\mathrm{a})-15E_2(a)\right]^2} \tag{25}$$

4. Stress intensity factor analysis of circumferential cracks in coke drums

In the following, the weight function derived in this paper will be used to calculate the stress intensity factor of a coke drum with circumferential cracks in a two-dimensional transient temperature field.

In order to verify the correctness of the method in this paper, the weight function derived by Meshii and Watanabe[12] is used to calculate the expression of the stress intensity factor, and the two are compared. The expression of the weight function proposed by Meshii and Watanabe[12] is as follows:

$$m(x;a)\left[\sqrt{\pi}a^2W\sqrt{a-x}\varphi_f F_M\right]=\sqrt{2}xF_M\left[W_x\varphi_f+2a(a-x)\frac{\partial\varphi_f}{\partial\varepsilon}\right]+(a-x)\times\left\{2a\varphi_f\left(\sqrt{2}x\frac{\partial F_M}{\partial\varepsilon}+(a-x)\frac{\partial V}{\partial\varepsilon}\right)+V\left[W(2a+x)\varphi_f+2a(a-x)\frac{\partial\varphi_f}{\partial\varepsilon}\right]\right\} \tag{26}$$

The calculation of the parameters involved is detailed in reference [12].

Now use the analytical method in Section 1 to derive the stress distribution of the coke drum on the imaginary crack surface when there is no crack.

When the internal pressure of the coke drum is not 0, the boundary condition of the problem can be considered to be fixed at the bottom, then:

$$x=0 \quad w_d=w_u \quad \frac{\partial w_d}{\partial x}=0 \tag{27}$$

The upper boundary condition is written as:

$$x=l \quad N_x=\frac{1}{2}q_zR \quad M_x=M_0 \quad N_{xz}=N_{xzo} \tag{28}$$

Among them, the values of M_0 and N_{xzo} are based on the height of the upper part of the coke drum using existing solutions[25].

At the liquid level, the continuity condition is met:

$$x=vt \quad w_d=w_u \quad \frac{\partial w_d}{\partial x}=\frac{\partial w_u}{\partial x} \quad M_d=M_u \quad N_{xzd}=-N_{xzu} \tag{29}$$

According to the above boundary conditions and liquid surface continuity conditions, the stress on the imaginary crack surface of the coke drum can be obtained, and the stress can be determined by the following expression:

$$\sigma_x=\frac{E}{1-\mu^2}\left[\left(\frac{du}{dx}-\frac{d^2w}{dx^2}\right)-(1+\mu)\alpha\Delta T(x,z,t)\right] \tag{30}$$

Among them, α is the thermal expansion coefficient of the coke drum wall material, ΔT is the temperature change of the coke drum wall, and u is the axial displacement of the cylindrical shell midplane. The expression of w is obtained from w_u or f using the specific position of the calculated point.

Calculate σ_x according to formula (30), and substitute formula (24) to calculate the corresponding stress intensity factors.

4.1 Stress intensity factors of different height cracks

The geometric parameters, material parameters, and operating parameters of the coke drum are shown in Table 1 and Table 2. Considering the water inlet time is 2000s, the liquid rising speed is 2mm/s, that is, the liquid level is 4m.

First, analyze the change of stress intensity factor with crack height. The variation of SIF with crack height at different crack depths is shown in Figure 10-16. Present solution is the calculation result of the weight function in this paper, and Ref. [12] is the calculation result of the weight function proposed by Meshii and Watanabe[12].

It can be seen from Fig. 10 to Fig. 16 that when the crack depth is 2mm-14mm, the calculation results in this paper are more consistent with those calculated by Meshii, and the relative error between the two is no more than 8%. It can be seen that the change trend of the stress intensity factor is consistent with the stress change trend. The stress intensity factor reaches the peak value near the fixed end constraint and near the liquid level. We must pay special attention to the detection of cracks in this area in actual production and life. . Under the same parameters, the results of this paper are slightly smaller than those of Meshii and Watanabe[12].

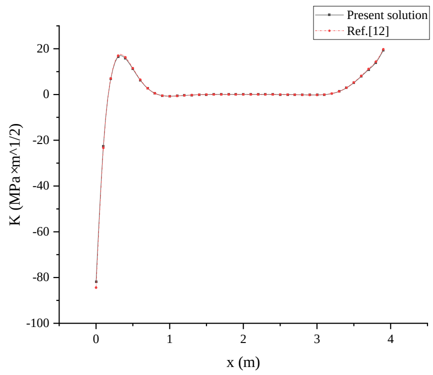

Fig.10 a=2mm

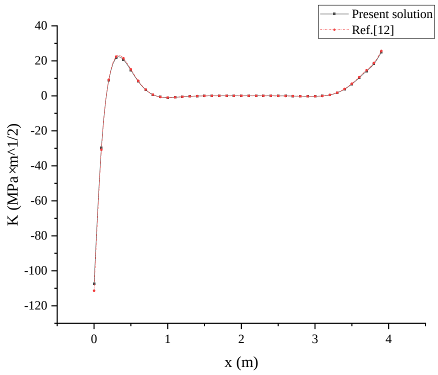

Fig.11 a=4mm

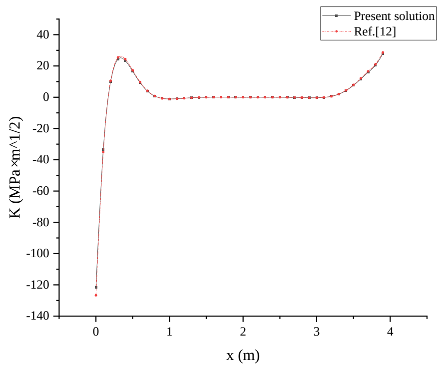

Fig.12 a=6mm

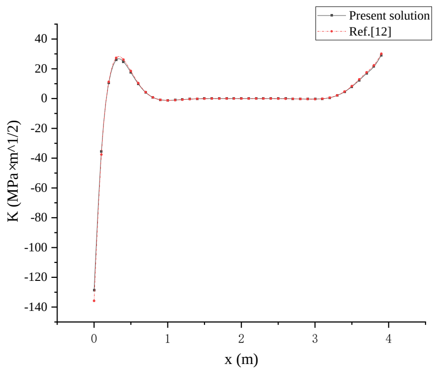

Fig.13 a=8mm

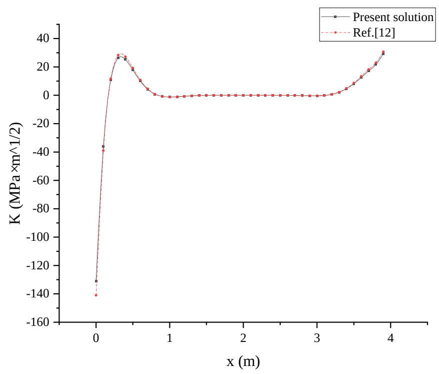

Fig.14 a=10mm

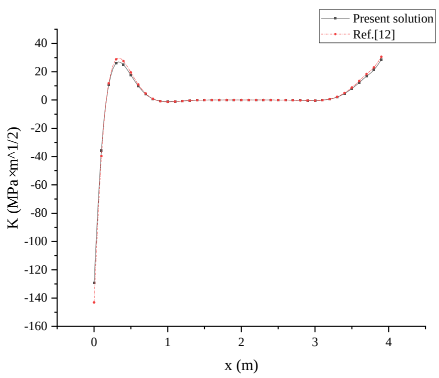

Fig.15 a=12mm

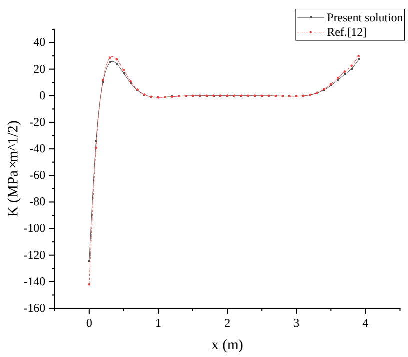

Fig.16 a=14mm

ISSN 2616-5767 Vol.4, Issue 8: 64-80, DOI: 10.25236/AJETS.2021.040808

The changes in the coke drum wall stress and strain field during the oil intake stage are similar to the changes in the water intake stage. The internal stress and strain field of the coke drum wall rises steadily with the increase of the oil level.

Figure 17-18 shows the stress field and stress intensity factor when the oil intake time is 4000s, the oil surface rise rate is 0.001m/s, that is, the oil surface height is 4m, and the crack depth is 10mm.

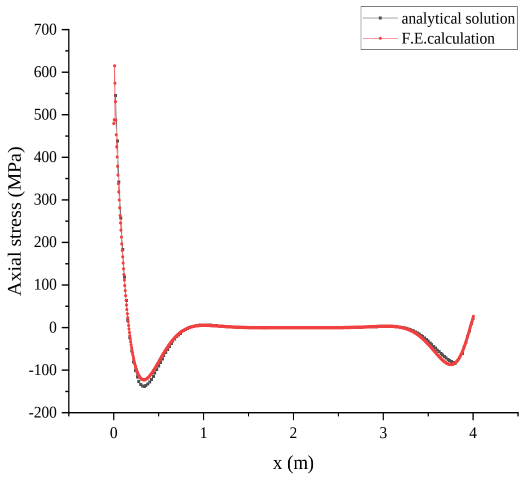

Fig.17 Changes of axial stress on the inner wall of coke drum with height

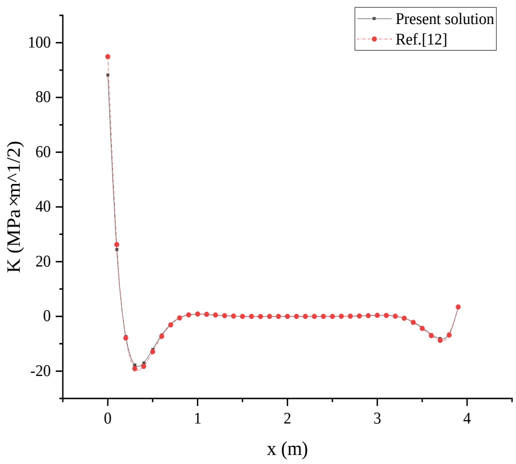

Fig.18 SIF change with crack height in hot feed filling step

Figure 17 shows the change in the axial direction of the inner wall of the coke drum when the oil level is at a height of 4m. It can be seen from the figure that the theoretical solution in this paper is more consistent with the finite element results. Figure 18 shows the change curve of the stress intensity factor with the height of the crack. Comparing Figure 17 and Figure 18, it is easy to see that the change trend of the stress intensity factor with the height of the crack is basically the same as the change trend of the axial stress of the coke drum inner wall with the height. Except for the fixed end of the bottom, there are two peaks of axial stress and stress intensity factor changing with height, one peak is located about 0.3m away from the bottom, and the other peak is located about 0.5m below the liquid surface. In the vicinity of the support, due to the strong restraint of the solid end of the coke drum bottom, the axial stress is relatively large, resulting in an increase in the stress intensity factor. It can be seen from Figure 18 that the results of this paper are in good agreement with the calculation results of the weight function derived by Meshii, and the maximum error does not exceed 6%. Similar to the results of the water intake stage, the results of this paper are greater than those of Meshii and Watanabe[12] under the same parameters.

In addition, it should be pointed out that, as shown in Figure 18, the stress intensity factor in the oil intake stage is negative (except at the end), while the stress intensity factors in the water intake stage in Figures 10-16 are all positive. This is because the coke drum wall under the liquid level shrinks due to the action of cold water in the water inlet stage, and thus is stretched by other parts, and its axial stress is tensile stress; while in the oil inlet stage, the coke drum wall is heated and expanded below the liquid level and is subjected to other parts. For partial compression, the axial stress is compressive stress. This indicates that crack arrest will occur during the oil intake stage, the stress intensity factor is negative, and the crack has a tendency to close.

4.2 The influence of liquid level rise on the stress intensity factor

The coke drum undergoes frequent thermal cycles during operation. At this time, the rising speed of the liquid in the coke drum is an important consideration. Different rising speeds of the liquid will inevitably bring about changes in the temperature field and the stress field. The following discusses the influence of the liquid rise rate on the stress intensity factor during the water inlet cooling stage. Considering that the cracks in the water inlet stage are located at the height of 2m and 1.9m in the coke drum, the wall material of the coke drum is 20g, the corresponding thermal conductivity is k=51.068W/(MK), and the liquid rise rate is 0.5mm/s, respectively. 0.8mm/s, 1mm/s, 2mm/s, 4mm/s, 8mm/s, assuming that the crack is located 0.1m below the liquid level, that is, the time for the liquid level to rise is 4200s, 2625s, 2100s, 1050s, 525s, 262.5 s.

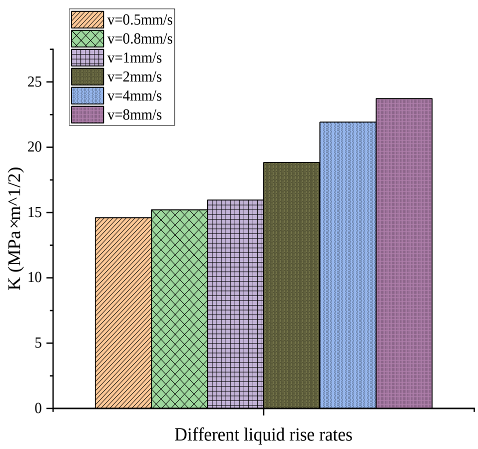

Fig.19 The crack is located at a height of 2m

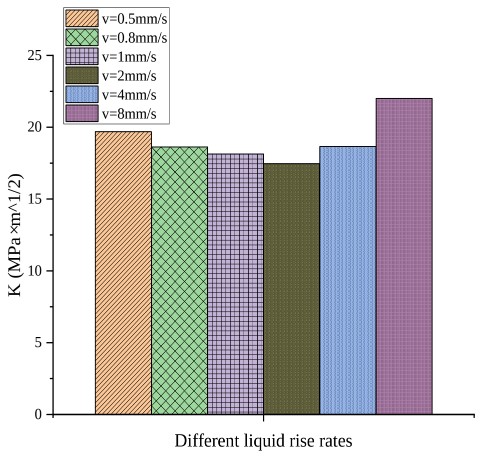

Fig.20 The crack is located at a height of 1.9m

ISSN 2616-5767 Vol.4, Issue 8: 64-80, DOI: 10.25236/AJETS.2021.040808

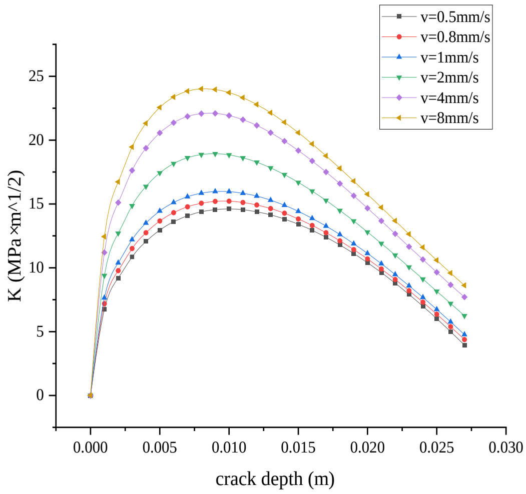

Fig.21 Stress intensity factors of different crack depths (crack position x=2m)

For Figure 19, as the liquid velocity increases, the crack stress intensity factor generally shows a gradually increasing trend. For different liquid velocities, the maximum stress intensity factor appears near the liquid surface, which is related to the change in stress. identical. For Figure 20, when the crack is located 0.1m below the liquid surface, the stress intensity factor at the liquid flow rate of 0.5mm/s is greater than the liquid flow rate of 0.8mm/s, 1mm/s, and 2mm/s. This is because when the flow rate is 0.5mm /s, the crack position is closer to the fixed end (1.9m), and the magnitude of the stress intensity factor is greatly affected by the constraints of the fixed end. Figure 21 reflects that when the crack depth exceeds 10mm (a/t=0.36), the stress intensity factor gradually decreases, and the crack has a tendency to arrest cracks at this time. This is consistent with the conclusion drawn by Meshii and Watanabe[12], which is further verified. The effectiveness of the weight function.

4.3 The influence of heat transfer parameters on the stress intensity factor

The thermal conductivity k of the coke drum material is also an important parameter that affects the crack propagation of the coke drum. In order to analyze the influence of the thermal conductivity k on the crack stress intensity factor, the coke drum wall material is 20g, AISI405 and 2-1/4Cr, and the corresponding heat conductivity The coefficients are: k=51.068 W/(M K), 35.861 W/(M K), 24.6 W/(M K), and other thermal performance parameters (such as specific heat capacity and density) remain unchanged. The cooling water rise rate is considered to be 2mm/s, and the water inlet time is 2000s; the hot oil rise rate is considered to be 1mm/s, and the oil inlet time is 4000s. The rising height of the liquid level during the water intake and oil intake stages is 4m.

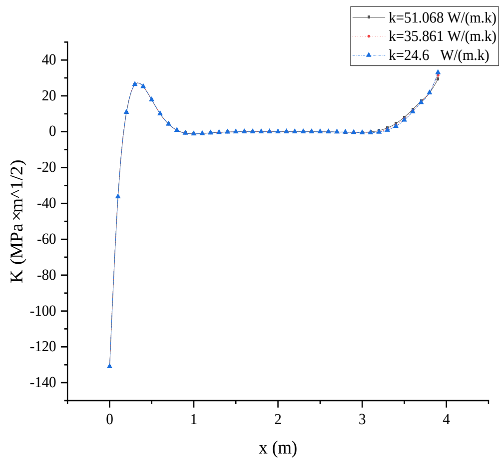

Fig.22 Stress intensity factor during water quench step

ISSN 2616-5767 Vol.4, Issue 8: 64-80, DOI: 10.25236/AJETS.2021.040808

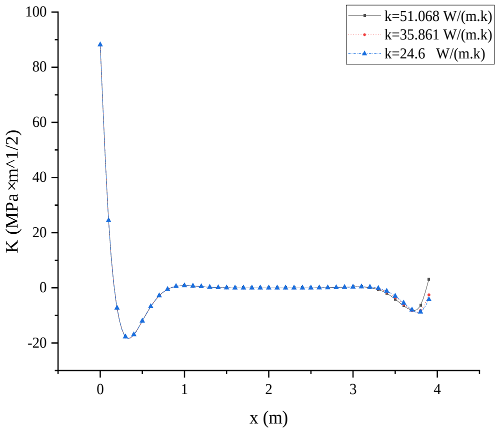

Fig.23 Stress intensity factor during hot feed filling step

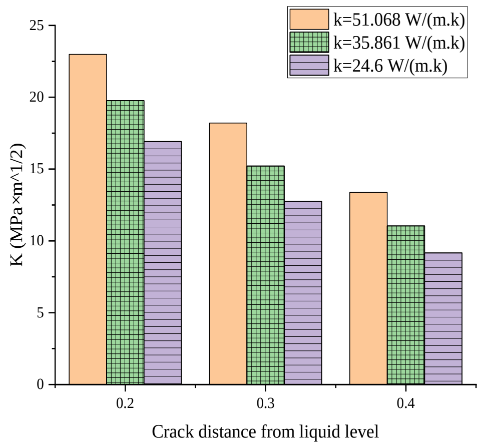

Fig.24 Stress intensity factor at a specific height during water quench step

For Figure 24, the stress intensity factors when the cracks are located at 0.2m, 0.3m, and 0.4m below the liquid level are selected. From Figure 22 to Figure 23, for different thermal conductivity coefficients, the first peak of the stress intensity factor appears Near the bottom of the coke drum, far away from the liquid level, the stress intensity factor is almost the same size, and near the liquid level, the smaller the k value, the greater the stress intensity factor. This situation occurs because when the liquid just arrives, the temperature of the inner wall of the coke drum rises or falls rapidly. The larger the thermal conductivity k, the faster the heat transfer speed along the radial direction of the coke drum, and the temperature of the wall near the inner wall of the coke drum The rate of change is faster, so the radial temperature space change rate near the inner wall of the coke drum is small, so that the radial temperature gradient value is smaller at the inner wall of the coke drum, and the axial stress of the inner wall of the coke drum changes relatively smoothly; and the thermal conductivity coefficient is small. The situation is just the opposite, so the axial stress on the inner wall of the coke drum changes relatively more.

5. Conclusion

(1) Based on the stress intensity factor of the edge crack of the finite width slab, combined with the self-consistent condition of the stress intensity factor and the curvature condition of the crack opening, a simple method is used to derive the weight function of the circumferential crack stress intensity factor of the thin-walled cylindrical shell.

(2) With the increase of crack depth, the stress intensity factor of the coke drum ring crack has a tendency to decrease. In this paper, the peak stress intensity factor occurs at a/t=0.36.

(3) This paper discusses the influence of liquid rise rate on crack stress intensity factor. It can be seen that under the premise that other thermal performance parameters (density and specific heat capacity)

remain unchanged, as the liquid velocity increases, the crack stress intensity factor generally shows a gradually increasing trend. In actual operation, we need to combine the actual As far as possible, use a relatively small liquid rise rate.

(4) For coke drums of different materials, different thermal conductivity coefficients also have a certain impact on the stress intensity factor. The smaller the thermal conductivity coefficient, the greater the maximum stress intensity factor. But overall, the effect of thermal conductivity on the stress intensity factor is not as great as that of the liquid rise rate.

(5) Accurate calculation of stress intensity factor is very important to predict crack growth and to perform reliable residual strength assessment of the coke drum structure. This paper calculates the stress intensity factors of cracks at different heights of the coke drum to predict the remaining life of the coke drum. Lay a certain theoretical foundation.

References

[1] Glinka G, Shen G(1991). Universal features of weight functions for cracks in mode I[J]. Engineering Fracture Mechanics, pp1135-1146.
[2] Nied H F, Erdogan F(1991). Transient thermal stress problem for a circumferentially cracked hollow cylinder [J]. Journal of thermal stresses,1983:1-14.
[3] Varfolomeyev I V, Petersilge M, Busch M(1998). Stress intensity factors for internal circumferential cracks in thin- and thick-walled cylinders[J]. Engineering Fracture Mechanics,pp491-500.
[4] Mettu S R, Forman R G(1993). Analysis of Circumferential Cracks in Circular Cylinders Using the Weight-Function Method.
[5] Nabavi S M, Ghajar R(2010). Analysis of thermal stress intensity factors for cracked cylinders using weight function method[J]. International Journal of Engineering Science,pp1811-1823.
[6] Xuan T(2018). Research on elastoplastic fracture mechanics behavior of thin-walled cylindrical shell with circumferential cracks[D]. Xi'an University of Architecture and Technology.
[7] Nied H F, Erdogan F(1983). Transient thermal stress problem for a circumferentially cracked hollow cylinder [J]. Journal of thermal stresses,pp1-14.
[8] Jayadevan K R(2002). Critical stress intensity factors for cracked hollow pipes under transient thermal loads [J]. Journal of thermal stress,pp951-968.
[9] Jones I S(2005). Impulse response model of thermal striping for hollow cylindrical geometries[J]. Theoretical and Applied Fracture Mechanics, pp77-88.
[10] Meshii T, Watanabe K(1998). Closed form stress intensity factor of an arbitrarily located inner-surface circumferential crack in an edge-restraint cylinder under linear radial temperature distribution[J]. Engineering Fracture Mechanics, pp519-527.
[11] Meshii T, Watanabe K(2001). Analytical Approach to Crack Arrest Tendency Under Cyclic Thermal Stress for an Inner-Surface Circumferential Crack in a Finite-Length Cylinder[J]. Journal of Pressure Vessel Technology Transactions of the Asme, pp220-225.
[12] Meshii T, Watanabe K(1999). Maximum stress intensity factor for a circumferential crack in a finite-length thin-walled cylinder under transient radial temperature distribution[J]. Engineering Fracture Mechanics, pp23-38.
[13] Meshii T, Watanabe K(2002). Stress Intensity Factor of a Circumferential Crack in a Thick-Walled Cylinder Under Thermal Striping[C]. Asme Pressure Vessels & Piping Conference. pp93-99.
[14] Meshii T, Watanabe K(2004). Normalized Stress Intensity Factor Range Solutions of an Inner-Surface Circumferential Crack in Thin- to Thick-Walled Cylinder under Thermal Striping by Semi-Analytical Numerical Method[J]. Journal of Thermal Stresses, ,pp253-267.
[15] Meshii T, Shibata K, Watanabe K(2006). Simplified method to evaluate upper limit stress intensity factor range of an inner-surface circumferential crack under steady state thermal striping[J]. Nuclear Engineering and Design, pp1081-1085.
[16] Nabavi S M, Shahani A R(2009). Thermal stress intensity factors for a cracked cylinder under transient thermal loading[J]. International Journal of Pressure Vessels & Piping, pp153-163.
[17] Iman, Eshraghi, Nasser, et al. Hyperbolic heat conduction based weight function method for thermal fracture of functionally graded hollow cylinders[J]. International Journal of Pressure Vessels & Piping, 2018.
[18] Fu J, Chen Z ,　Qian L , et al. Non-Fourier thermoelastic behavior of a hollow cylinder with an embedded or edge circumferential crack[J]. Engineering Fracture Mechanics, 2014.
[19] Ning Z.H, Liu R.H(2010). Analysis of transient temperature field in coke drums[J]. Applied Mathematics & Mechanics, pp.291-304.
[20] Ning Z.H, Liu R.H, Huang S Q , et al(2011). Analytical Solution of the Thermoelasticity Problem in

ISSN 2616-5767 Vol.4, Issue 8: 64-80, DOI: 10.25236/AJETS.2021.040808

a Coke Drum With Cladding[J]. Journal of Pressure Vessel Technology, p031201.
[21] Bueckner H F. Novel Principle for the Computation of Stress Intensity Factors[J]. Z.angew. math. mech, 1970.
[22] Rice J R(1972). Some remarks on elastic crack-tip stress fields[J]. International Journal of Solids & Structures, pp751-758.
[23] China Academy of Aeronautics and Astronautics. Handbook of Stress Intensity Factors-Revised Edition[M]. Science Press, 1993.
[24] Zhao X.C, Wu X.R, Tong D(2018).H. Accurate analytical weight function solutions for crack at edge of circular hole in infinite plate [J]. Journal of Aeronautics, p12.
[25] Liu R.H. Plate and Shell Mechanics [M]. Beijing: Mechanical Industry Press, 1990.